

ENGINEERING DESIGN OF THE LUX PHOTOINJECTOR*

J. W. Staples, S. P. Virostek and S. M. Lidia, LBNL, Berkeley CA 94720 USA

Abstract

The photoinjector for the LBNL LUX project, a femtosecond-regime X-ray source, is a room-temperature 1.3 GHz 4 cell structure producing a 10 MeV, nominal 30 psec, 1 nanocoulomb electron bunch at a 10 kHz rate. The first cell is of reentrant geometry, with a peak field of 64 MV/m at the photocathode surface, the geometry of which will be optimized for minimum beam emittance. The high repetition rate and high peak power results in a high average surface power density. The design of the cavity, its cooling structure and power couplers, is coordinated with the configuration of the RF system, including a short, high-power driving pulse and active removal of stored energy after the beam pulse to reduce the average power dissipated in the cavity. An RF and thermal analysis of the photoinjector will be presented.

REDUCING AVERAGE CAVITY POWER

The design of the cavity shape is dictated by requirements of maximizing the shunt impedance to minimize the RF power requirement for high duty factor operation, as well as optimizing the field profile to provide a 20-30 picosecond, 1 nanocoulomb beam pulse with an emittance of less than 2π mm-mrad [1]. The reentrant structure with rounded corners minimizes the peak electric fields to 94 MV/m with 64 MV/m at the photocathode surface.

The LUX photoinjector presents severe problems in thermal management. The dissipated cavity wall power at full gradient with 64 MV/m at the photocathode is 833 kW, corresponding to an unloaded Q_0 of 19000, 85% of pure copper Q_0 . The filling time with unity coupling is 2.34 microseconds. A 5 microsecond pulse will fill the cavity to 88% gradient at unity coupling, so the input power must be raised to $(1/0.88)^2 = 1.29$ times 833 kW, or 1075 kW to bring the cavity to full gradient at the end of 5 microseconds. At a 10 kHz repetition rate, the total cavity dissipation is 31.3 kW, with peak wall power densities as high as 98 W/cm². Figure 1 shows the wall power density in an URMEL [2] calculation with a 5 microsecond RF pulse at 10 kHz and unity coupling coefficient β to the klystron.

Three ways are presented to reduce the cavity wall power density:

- Reduce the pulse length and increase the peak power.
- Increase the coupling β to the RF source to reduce the filling time.
- Actively remove the stored energy in the cavity.

*This work was supported by the U.S. Department of Energy under Contract No. DE-AC03-76SF00098

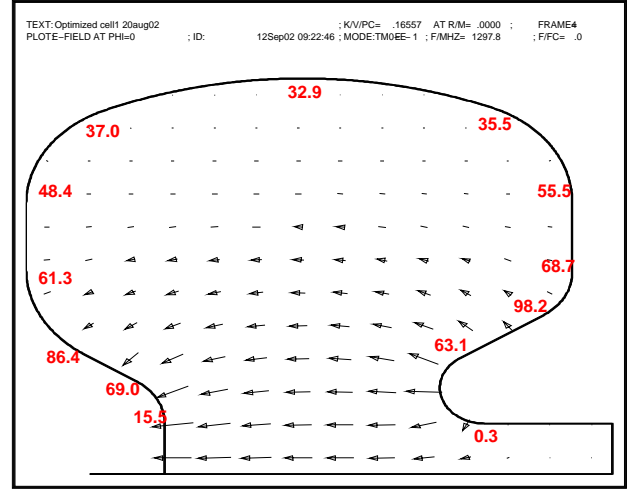


Figure 1: Cavity Wall Power Density, Watts/cm², see text

Each of these techniques will increase the peak power required of the klystron and the power dissipated in the dummy load of the circulator between the klystron and the cavity, but the reduction in cavity power is significant.

The power dissipated in the cavity and the dummy load terminating the third port of the circulator, as well as the required klystron power are calculated in the same manner as for a SLED configuration [3]. The fields from the klystron, and emitted from the stored energy are E_k and E_e respectively, where the power reflected from the cavity is $P_L = E_e^2/\beta$ and the power reflected back to the dummy load is proportional to $(E_e + E_k)^2$. A first-order differential equation results:

$$\tau \frac{dE_e(t)}{dt} + E_e(t) = -\frac{2\beta}{1+\beta} E_k(t) \quad (1)$$

where τ is the loaded cavity filling time.

A code has been written to solve the above equation for various values of the klystron pulse length, rise-time and phase, and input coupling constant β . Figure 2 shows the output with the cavity field in black, reflected field in red, and klystron field in blue. Each power is proportional to the square of the field level. Table 1 lists the average power dissipated in the walls of the cavity for RF pulse lengths of 2 through 5 microseconds with a coupling factor β of 1 through 3 to the klystron. The klystron power is adjusted to raise the field at the photocathode to 64 MV/m at the end of the pulse, and increasing the coupling reduces the filling time. For these short RF pulses, the waveguide-cavity coupling constant β has only a small effect on the average power dissipated in the cavity. Reducing the pulse length has a larger effect. However, the price to be paid is a higher

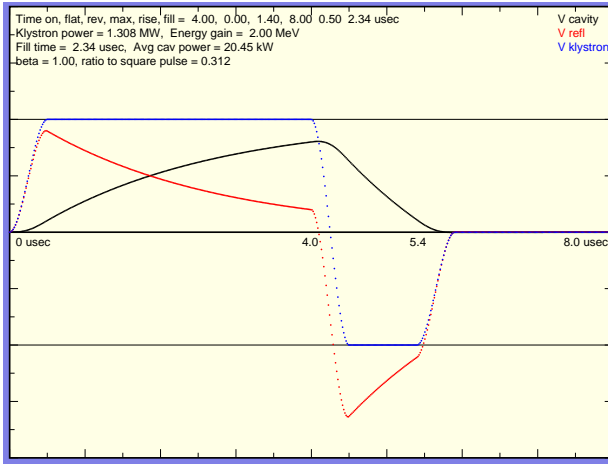


Figure 2: Cavity, Reflected, Klystron fields vs. time

pulse lth	$\beta = 1$	$\beta = 2$	$\beta = 3$
2 μsec	16.5 kW	13.9 kW	13.0 kW
3 μsec	20.9	19.1	18.8
4 μsec	25.8	25.1	25.6
5 μsec	31.3	31.7	33.0

Table 1: Average Cavity Power (kW) vs. pulse length, β

klystron peak power requirement and a higher peak power reflected to the dummy load through the circulator. Table 2 lists the peak klystron power required. For all but the 2

pulse lth	$\beta = 1$	$\beta = 2$	$\beta = 3$
2 μsec	2.52 MW	1.80 MW	1.66 MW
3 μsec	1.60	1.29	1.30
4 μsec	1.24	1.10	1.19
5 μsec	1.07	1.02	1.14

Table 2: Peak klystron power vs. pulse length, β

microsecond pulse, the peak klystron power is minimized at $\beta = 2$, as reflected power from mismatch is more than compensated for by the shorter filling time, reducing the forward power needed to attain the required gradient at the end of the pulse.

One more stratagem is available to further reduce the power dissipation in the cavity. Using a SLED technique, the phase of the RF drive may be reversed, actively removing the stored energy from the cavity after the beam pulse from the photoinjector, and dissipating it in the dummy load. The price to be paid is a longer klystron pulse and higher average and peak dummy load power. The length of the extended and phase-flipped pulse is determined by the time necessary to remove the cavity stored energy at the given coupling constant β . Figure 2 shows the klystron phase flipped at the end of the cavity fill, with the cavity field reduced faster than the normal filling time. Table 3 shows the average cavity power dissipated with optimal phase flip time to reduce the stored energy to zero. The increased pulse length increases the average klystron power by about a third. The large spike in reflected power may

pulse lth	$\beta = 1$	$\beta = 2$	$\beta = 3$
2 μsec	9.40 kW	9.50 kW	9.70 kW
3 μsec	14.2	14.9	15.7
4 μsec	19.5	20.9	22.5
5 μsec	25.2	27.7	30.0

Table 3: Average Cavity Power with Phase Flip

be reduced by slowing the transition to the reversed phase from the klystron. Figure 2 shows a 4 microsecond fill with a 0.5 microsecond klystron rise and phase flip time and a 1.4 microsecond extension of the klystron pulse in the energy removal period. As the table shows, the effect of the coupling constant β is weak, and therefore the trimming to a specific value of coupling constant of the iris coupler after manufacture may be eliminated entirely.

ANSYS ANALYSIS OF THERMAL LOAD

A finite element analysis has been carried out to characterize the electromagnetic, thermal and structural behavior of the photoinjector cavity subject to the prescribed RF loading. A single ANSYS [4] model has been developed to perform all of the calculations using a multi-step process [5]. To facilitate adjustments to the cavity geometry, all FEA solid modeling is accomplished using fully parametric input files.

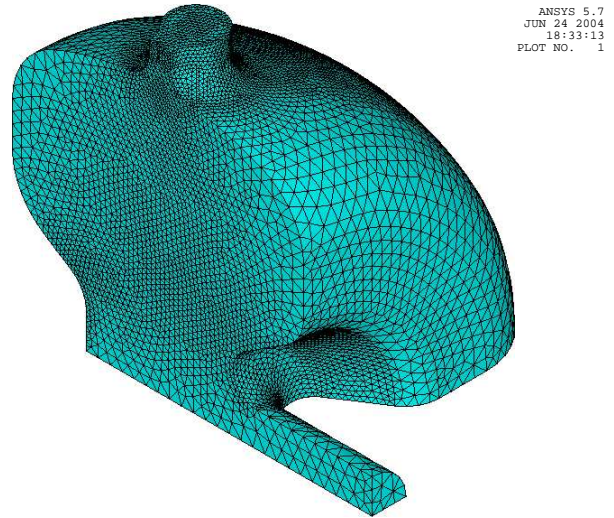


Figure 3: Element Plot of Quarter-Symmetry RF Model

The first phase of the analysis consists of performing a high frequency electromagnetic analysis of the cavity vacuum volume. The model is constructed to take advantage of the four-fold symmetry of the cavity about the beam axis. The volume is meshed with tetrahedral RF elements (HF119) with a finer mesh in areas of high fields and a coarser mesh in the other areas of the cavity. By appropriately controlling the mesh density, an accurate solution for the magnetic fields at the surface (and thus the surface heat flux) is obtained while minimizing the run time and mem-

ory requirements. Figure 3 shows the meshed model used to generate the electromagnetic solution.

Electric wall boundary conditions are applied to the exterior of the vacuum volume model only on those surfaces that represent the cavity wall-to-vacuum interface. An impedance boundary condition is also applied to these areas in the form of the cavity surface resistance. Including the impedance condition in the analysis allows ANSYS to compute the theoretical Q value for the cavity. No boundary conditions are applied to the model symmetry planes as these surfaces default to magnetic walls.

The RF solution is obtained as a modal analysis of the cavity. ANSYS calculates the resonant frequency of the cavity, and, by specifying that the modes are to be “extracted”, the element results are available as well in the form of E and H field data. In a modal solution, the field results are arbitrarily normalized and will require scaling in order to allow calculation of the surface heat fluxes. A macro is used to read in the H field solution at each surface node and calculate the resulting heat flux based on the surface resistance, the element areas and a scale factor derived from the expected total power loss in the cavity, 31 kW in this case. The heat fluxes are applied to the nodes of a new surface mesh that matches node-for-node the mesh on the surface of the RF model. The surface mesh consists of surface effect elements (SURF152) without mid-side nodes and with heat flux loading capability.

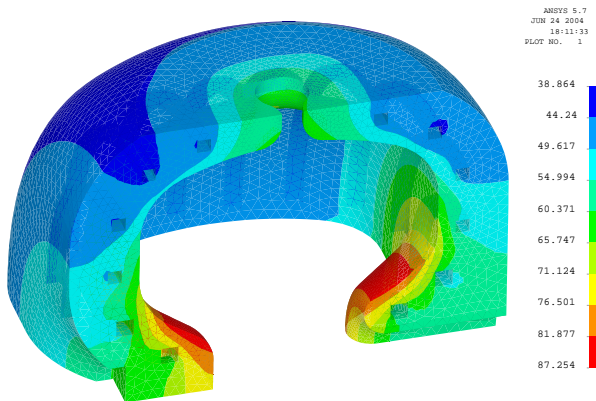


Figure 4: Cavity Thermal Model and Resulting Temperature Contours

The thermal analysis of the photoinjector cavity begins by deleting the original RF elements, leaving only the new surface elements with the applied heat fluxes. Next, a solid model representing the actual cavity walls (as opposed to the vacuum region) is constructed around the existing surface elements. All relevant features of the cavity are included, such as cooling passages, ports and beam tube connections. Upon meshing the new solid volume with the appropriate thermal elements, the heat flux loads are automatically transferred to the model. Heat balance is achieved in the model by applying convective cooling to the surfaces of the water passages. The cavity model and the resulting

temperature contours for 20°C cooling water are shown in Figure 4.

ANSYS allows direct solution of the structural problem by means of converting the thermal elements to their equivalent structural elements. The temperature data obtained from the thermal solution is applied as a load on the structural model. Vacuum loads, symmetry boundary conditions and cavity support constraints are applied as well. The peak von Mises stress in the photoinjector was found to be approximately 65 Mpa (Figure 5).

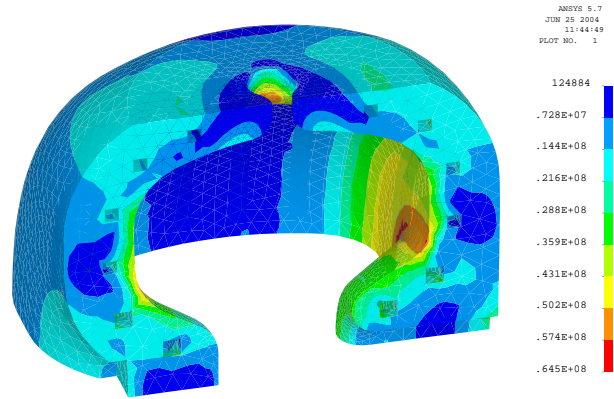


Figure 5: Cavity Structural Model and Resulting Stress Contours

The displacements of the cavity walls due to the loading conditions, including thermal distortion, are obtained from the structural solution as well. The nodal displacements at the cavity-to-vacuum interface, taken at the symmetry plane not containing the iris coupler, are added to the original nodal locations to yield a 2-D profile of the displaced cavity shape. A new RF model based on the displaced profile can be used to predict changes in cavity frequency due to various loading and thermal conditions. As a verification of this procedure, the same model was run through the entire RF, thermal and structural solution with the only change being to the cooling water temperature. The resulting frequency shift was -23.0 kHz per °C change in water temperature. This value agrees to within 0.5% of the expected sensitivity obtained from the product of the nominal cavity frequency and the coefficient of thermal expansion of the cavity material.

REFERENCES

- [1] S. M. Lidia, Design of Injector Systems for LUX, this conference
- [2] U. Lausroer et al, DESY M-87-03
- [3] Z. Farkas et al, SLAC-PUB-1453, June 1974
- [4] ANSYS is a registered trademark of SAS IP, Inc.
- [5] N. Hartman and R.A. Rimmer, “Electromagnetic, Thermal, and Structural Analysis of RF Cavities using ANSYS”, PAC 2001.